

# Broadband degenerate OPO for mid-infrared frequency comb generation

Nick Leindecker,\* Alireza Marandi,  
Robert L. Byer, and Konstantin L. Vodopyanov

*E.L. Ginzton Laboratory, Stanford University, Stanford CA, 94305, USA*  
*\*nick.leindecker@stanford.edu*

**Abstract:** We present a new technique suitable for generating broadband phase- and frequency-locked frequency combs in the mid-infrared. Our source is based on a degenerate optical parametric oscillator (OPO) which rigorously both down-converts and augments the spectrum of a pump frequency comb provided by a commercial mode-locked near-IR laser. Low intracavity dispersion, combined with extensive cross-mixing of comb components, results in extremely broad instantaneous mid-IR bandwidths. We achieve an output power of 60 mW and 20dB bandwidth extending from 2500 to 3800 nm. Among other applications, such a source is well-suited for coherent Fourier-transform spectroscopy in the absorption-rich mid-IR ‘molecular fingerprint’ region.

©2011 Optical Society of America

**OCIS codes:** (190.4975) Parametric processes; (190.4410) Nonlinear optics, parametric processes.

---

## References and links

1. F. Keilmann, C. Gohle, and R. Holzwarth, “Time-domain mid-infrared frequency-comb spectrometer,” *Opt. Lett.* **29**(13), 1542–1544 (2004).
2. F. Adler, P. Maslowski, A. Foltynowicz, K. C. Cossel, T. C. Briles, I. Hartl, and J. Ye, “Mid-infrared Fourier transform spectroscopy with a broadband frequency comb,” *Opt. Express* **18**(21), 21861–21872 (2010).
3. P. B. Corkum, and F. Krausz, “Attosecond science,” *Nat. Phys.* **3**(6), 381–387 (2007).
4. C. M. S. Sears, E. Colby, R. J. England, R. Ischebeck, C. McGuinness, J. Nelson, R. Noble, R. H. Siemann, J. Spencer, D. Walz, T. Plettner, and R. L. Byer, “Phase stable net acceleration of electrons from a two-stage optical accelerator,” *Phys. Rev. Lett.* **11**, 101301 (2008).
5. E. Sorokin, I. T. Sorokina, J. Mandon, G. Guelachvili, and N. Picqué, “Sensitive multiplex spectroscopy in the molecular fingerprint 2.4  $\mu\text{m}$  region with a  $\text{Cr}^{2+}:\text{ZnSe}$  femtosecond laser,” *Opt. Express* **15**(25), 16540–16545 (2007).
6. C. L. Hagen, J. W. Walewski, and S. T. Sanders, “Generation of a continuum extending to the midinfrared by pumping ZBLAN fiber with an ultrafast 1550-nm source,” *IEEE Photon. Technol. Lett.* **18**(1), 91–93 (2006).
7. C. Langrock, M. M. Fejer, I. Hartl, and M. E. Fermann, “Generation of octave-spanning spectra inside reverse-photon-exchanged periodically poled lithium niobate waveguides,” *Opt. Lett.* **32**(17), 2478–2480 (2007).
8. R. A. Kaindl, M. Wurm, K. Reimann, P. Hamm, A. M. Weiner, and M. Woerner, “Generation, shaping, and characterization of intense femtosecond pulses tunable from 3 to 20  $\mu\text{m}$ ,” *J. Opt. Soc. Am. B* **17**(12), 2086–2094 (2000).
9. C. Erny, K. Moutzouris, J. Biegert, D. Kühlke, F. Adler, A. Leitenstorfer, and U. Keller, “Mid-infrared difference-frequency generation of ultrashort pulses tunable between 3.2 and 4.8  $\mu\text{m}$  from a compact fiber source,” *Opt. Lett.* **32**(9), 1138–1140 (2007).
10. A. Gambetta, R. Ramponi, and M. Marangoni, “Mid-infrared optical combs from a compact amplified Er-doped fiber oscillator,” *Opt. Lett.* **33**(22), 2671–2673 (2008).
11. J. H. Sun, B. J. S. Gale, and D. T. Reid, “Composite frequency comb spanning 0.4–2.4  $\mu\text{m}$  from a phase-controlled femtosecond Ti:sapphire laser and synchronously pumped optical parametric oscillator,” *Opt. Lett.* **32**(11), 1414–1416 (2007).
12. F. Adler, K. C. Cossel, M. J. Thorpe, I. Hartl, M. E. Fermann, and J. Ye, “Phase-stabilized, 1.5 W frequency comb at 2.8–4.8  $\mu\text{m}$ ,” *Opt. Lett.* **34**(9), 1330–1332 (2009).
13. D. Brida, C. Manzoni, G. Cirimi, M. Marangoni, S. De Silvestri, and G. Cerullo, “Generation of broadband mid-infrared pulses from an optical parametric amplifier,” *Opt. Express* **15**(23), 15035–15040 (2007).
14. J. Falk, “Instabilities in the doubly resonant parametric oscillator: a theoretical analysis,” *IEEE J. Quantum Electron.* **7**(6), 230–235 (1971).

15. C. D. Nabors, S. T. Yang, T. Day, and R. L. Byer, "Coherence properties of a doubly-resonant monolithic optical parametric oscillator," *J. Opt. Soc. Am. B* **7**(5), 815–820 (1990).
  16. S. T. Wong, T. Plettner, K. L. Vodopyanov, K. Urbanek, M. Dignonet, and R. L. Byer, "Self-phase-locked degenerate femtosecond optical parametric oscillator," *Opt. Lett.* **33**(16), 1896–1898 (2008).
  17. S. T. Wong, K. L. Vodopyanov, and R. L. Byer, "Self-phase-locked divide-by-2 optical parametric oscillator as a broadband frequency comb source," *J. Opt. Soc. Am. B* **27**(5), 876–882 (2010).
  18. K. L. Vodopyanov, N. C. Leindecker, R. L. Byer, and V. Pervak, "More Than 1000-nm-wide Mid-IR Frequency Comb Based on Divide-by-2 Optical Parametric Oscillator", CLEO/QELS 2010 Conference, Opt. Soc. Amer., paper CThH5 (2010).
  19. A. Yariv, *Quantum Electronics*, 3rd ed. (Wiley, New York 1988).
  20. A. Marandi, N. Leindecker, R. L. Byer, and K. L. Vodopyanov, "Coherence properties of a mid-infrared frequency comb produced by a degenerate optical parametric oscillator," CLEO/QELS 2011 Conference, Opt. Soc. Amer., paper QtuF2 (2011).
- 

## 1. Introduction

The broadband and coherent nature of frequency combs produced in the visible and near-infrared – both in frequency (a manifold of equally spaced narrow frequency-comb lines) and in time (a strictly periodic train of pulses with stable carrier-envelope phase) – has allowed a revolution in precision metrology. Extending the operating range of optical frequency combs to wavelengths  $> 2 \mu\text{m}$  is advantageous for a wide range of applications including coherent molecular spectroscopy and trace gas detection in the 'fingerprint' region [1,2], attosecond physics [3], and laser-driven particle acceleration [4]. However, the extension of frequency comb sources to the mid-infrared (mid-IR) has remained technically challenging. Recent methods include direct laser sources [5], supercontinuum generation in optical fibers [6] and engineered  $\chi^{(2)}$  nonlinear optical devices [7], optical rectification [8], difference-frequency generation [9,10] optical parametric oscillators (OPOs) [11,12] and amplifiers [13].

From the early days of nonlinear optics, it was understood that a degenerate OPO is an over-constrained and inherently unstable system [14]. However, it has since been shown that a degenerate OPO is a nearly ideal phase-locked frequency divider for single-frequency CW radiation [15]. Extending on our earlier demonstration of a self-phase-locked broadband near-IR subharmonic OPO pumped by a Ti:Sapphire laser [16,17] this work shows that with proper design, a synchronously-pumped frequency-divide-by-two OPO proves equally useful for transposing near-IR frequency combs to the mid-infrared.

Operated at degeneracy, our OPO provides broad instantaneous bandwidth. In fact, massive cross mixing within the manifold of comb lines not only provides phase- and frequency- locking of the mid-IR comb lines to the pump, but also results in enhanced bandwidth relative to the pump [17]. Salient features of our approach include: (i) simplicity of the setup, (ii) low ( $< 100 \text{ mW}$ ) pump power requirement, (iii) potential for high ( $> 90\%$ ) conversion efficiency and (vi) possibility of achieving more-than-octave-wide spectrum due to the wide acceptance bandwidth of the parametric conversion process near degeneracy.

## 2. Methods

A schematic overview of our OPO system is presented in Fig. 1. The pump is a 1560-nm mode-locked erbium-fiber laser from Menlo Systems (C-fiber model, repetition frequency 100 MHz, pulse duration 70 fs, average power 300 mW) or from Toptica Photonics (FemtoFiber Pro model, repetition frequency 80 MHz, pulse duration 85 fs, average power 380 mW). The resonator [18] is a 3-m (or 3.75-m) -long ring cavity which is matched in length to the pump repetition rate. Both Menlo and Toptica pump lasers have been used with equal success. The intracavity optics comprise a flat dielectric mirror  $M_1$  with high transmission ( $>75\%$ ) for the pump and high reflectivity in the 2400–4200-nm range, and 5 gold coated mirrors  $M_2 - M_6$  with high (98.7%) mid-IR reflection. Mirrors  $M_2$  and  $M_3$  are concave with radius of curvature  $\text{ROC}=50 \text{ mm}$ , and mirrors  $M_4 - M_6$  are flat. Broadband gain centered at 3120 nm is provided by a short, 0.5-mm (or 0.2-mm) MgO-doped periodically poled lithium niobate (MgO:PPLN) crystal from Crystal Technology Inc. with an aperture

1x8 mm. The crystal was cut such that the interacting beams propagate perpendicular to the inverted domain boundaries when the beam enters the crystal at the Brewster angle. The domain reversal period is 34.8  $\mu\text{m}$  and designed for type-0 ( $e=e+e$ ) phase matched subharmonic generation (1560  $\rightarrow$  3120nm) at a temperature of 32°C. With this poling period, our PPLN crystal length amounts to only 14 (or 6) quasi phase matching domain reversal periods.

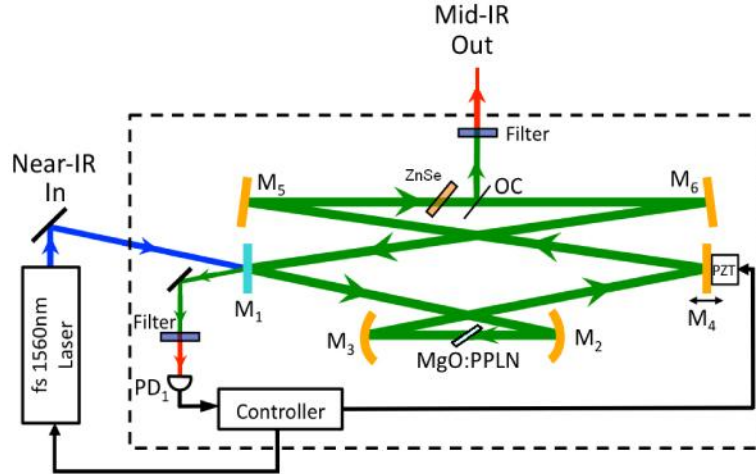


Fig. 1. Schematic of the ring-cavity OPO setup. Here  $M_1$  is a dielectric mirror for in-coupling of the pump,  $M_2$  and  $M_3$  are concave and  $M_4$ - $M_6$  are flat gold-coated mirrors,  $PD_1$  is an InAs detector, the filter is a Ge-based long pass ( $> 2.5 \mu\text{m}$ ) filter, OC is a pellicle outcoupler, and PZT is a piezo actuator stage.

Our ring cavity produces an eigenmode with a calculated  $w=15 \mu\text{m}$  ( $1/e^2$  intensity radius) beam waist inside the PPLN crystal. For near optimal mode matching, the pump laser beam is conditioned by a reducing telescope to a diameter and wave front curvature before mirror  $M_1$  such that after reflecting from short focal length mirror  $M_2$  its waist inside the PPLN crystal was approximately  $w=11 \mu\text{m}$ , approximating a 'confocal' pumping condition.

Astigmatism inside the OPO cavity, caused by slightly oblique ( $4^\circ$ ) incidence on the mirrors  $M_2$  and  $M_3$  is compensated by opposite-sign astigmatism of the Brewster angle PPLN crystal. As a result, the calculated beam ellipticity  $(a-b)/a$  (where  $a$  and  $b$  are the beam radii in two orthogonal planes) is substantially reduced: 4% for 0.5-mm PPLN and 20% for 0.2-mm-long PPLN. The inset to Fig. 3 shows the near circular experimental beam shape for the 0.5-mm crystal.

An additional 0.9-mm to 3-mm thick plane-parallel plate of ZnSe having positive ( $148 \text{ fs}^2/\text{mm}$ ) group velocity dispersion (GVD) at 3120 nm is inserted inside the cavity at Brewster angle to compensate the negative GVD of PPLN ( $-583 \text{ fs}^2/\text{mm}$ ). The output is extracted with a 2- $\mu\text{m}$ -thick pellicle beam splitter having  $R \sim 8\%$  reflection over a broad bandwidth.

Oscillation occurs when signal/idler waves are brought into simultaneous resonance near degeneracy by fine-tuning the cavity length with the piezo stage (PZT) attached to  $M_4$ . Several of these resonances occur, separated by  $\lambda/2$  ( $\sim 1.56 \mu\text{m}$ ) increments in the roundtrip cavity length (Fig. 2), where  $\lambda$  is the central wavelength [17]. For some measurements, the OPO was operated in a 'ramp mode' where the intracavity piezo actuator was driven with a linear ramp of  $10 \mu\text{m}$  (roundtrip length variation  $20 \mu\text{m}$ ), tuning the OPO sequentially through several resonances as shown. Continuous operation of the OPO is achieved by locking its cavity length to one of the resonances with a simple locking circuit. The circuit imposes a small frequency dither on the pump laser oscillator (via piezo translation of an intracavity mirror). The output of the OPO thus exhibits slight intensity modulation which is monitored by an InAs detector  $PD_1$  (Fig. 1) and demodulated in a phase sensitive detector

referenced to the pump dither signal. The average DC level from the phase detector indicates whether the OPO resonator needs to be tuned shorter or longer for higher conversion. This signal is passed through a loop filter to create a suitable error signal for driving a high voltage amplifier connected to the piezo actuator supporting  $M_4$ .

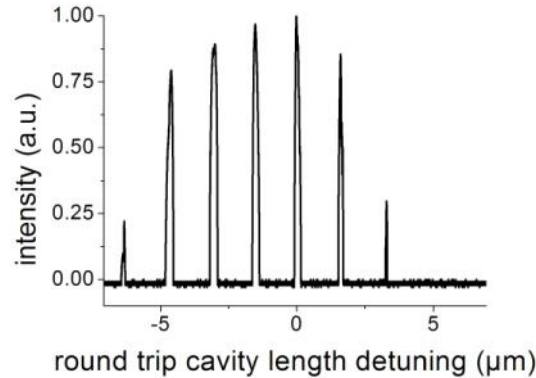


Fig. 2. OPO output power as a function of cavity length, revealing a number of discrete oscillation peaks.

### 3. Results

When operated with minimum roundtrip loss, estimated to be 10-20% due chiefly to absorption in the cavity mirrors, we observed an OPO threshold of 28 mW average pump power for the 0.5-mm PPLN crystal, and 65 mW for the 0.2-mm PPLN. As expected for a doubly-resonant OPO [19], the threshold was found to scale as the *square* of total intracavity loss, which we verified by adding intracavity loss in a controllable fashion and measuring the resulting threshold. As pump power increased, oscillation begins to occur at adjacent discrete length detunings. At full pump power, we observe oscillation at seven discrete lengths, as in Fig. 2. With an outcoupling of 8%, 300mW of pump power, and a 0.5-mm PPLN crystal, we recorded 82% pump depletion and extracted 60mW average power corresponding to 40% quantum conversion efficiency.

The OPO output spectrum was measured using an  $f = 20\text{cm}$  monochromator equipped with a 100 line/mm diffraction grating. Mid-IR light passing through the monochromator was detected using a photovoltaic mercury cadmium telluride (1-12  $\mu\text{m}$ ) detector which was cooled to 77K. For greater convenience, a thermoelectrically cooled photoconductive InSb detector was occasionally substituted. A long pass filter on germanium substrate was used to reject residual 1560nm pump. The broadest output bandwidth we have measured extends from 2500 to 3800 nm at a level 20 dB below the peak value. Figure 3 shows the spectrum of the OPO containing 0.5-mm PPLN crystal both with (black curve) and without (gray curve) a 2-mm ZnSe plate used as a 2<sup>nd</sup> order GVD compensator. One can clearly see that the spectrum becomes broader with ZnSe for GVD compensation. Shown in the inset is the near-IR pump laser spectrum, taken with an Agilent optical spectrum analyzer (OSA). The shape and width of the output spectrum was found to depend significantly on which of the discrete resonant cavity-length peaks the OPO is tuned. In agreement with theoretical expectations [17], the output spectrum was found to narrow at lower pump power and/or increased outcoupling. The width of the spectrum obtained with the 0.2-mm PPLN was similar (within 10%) to that observed with the 0.5-mm-long PPLN.

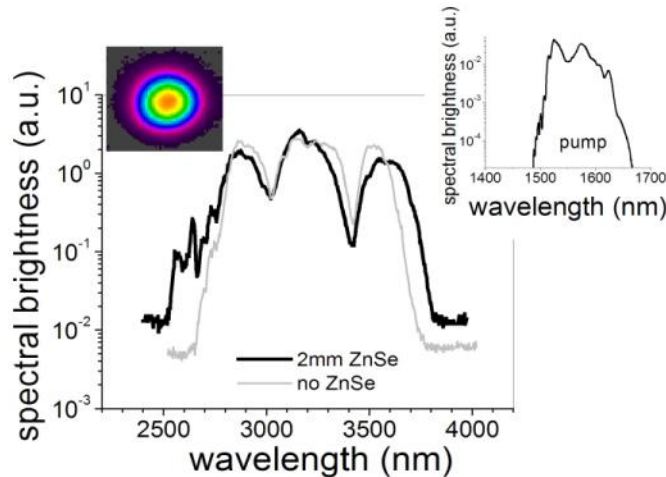


Fig. 3. Mid-IR OPO spectrum measured with a monochromator both with (black curve) and without (gray curve) 2nd -order GVD compensation using a ZnSe plate inside the cavity. Insets show the far-field mid-IR beam profile taken with a Pyrocam III Spiricon camera and the pump laser spectrum taken with an OSA.

Our calculations show that the OPO spectral band is mainly limited by (i) intracavity group delay dispersion and (ii) finite bandwidth of parametric gain. The calculated extra phase accumulated per cavity roundtrip, due to combined group delay dispersion of the 0.5-mm-long PPLN plus mirrors, is shown on Fig. 4 (gray curve). This is compared to the case when a 2-mm ZnSe GVD-compensating plate was added (Fig. 4, black curve). The two horizontal lines represent the tolerance for phase deviation ( $\pm 0.2$  rad) which was calculated [17] taking into account cavity finesse and the pumping strength in terms of times above threshold. Also shown on this plot (dashed line) is parametric gain curve for the 0.5-mm PPLN crystal. The maximum spectral band obtained from theoretical considerations is in good agreement with the experimentally observed band of 2500-3800 nm ( $\Delta\nu = 1370$   $\text{cm}^{-1}$ ). This bandwidth exceeds the 20-dB-level pump spectral width, expressed in frequency units, by approximately by a factor of two.

Despite of the smaller group delay dispersion contribution and larger parametric gain bandwidth for the shorter (0.2-mm) PPLN, we preferred to work with the 0.5-mm crystal because of the lower OPO threshold. However with more pump power available, we expect to access greater bandwidth with shorter PPLN crystals.

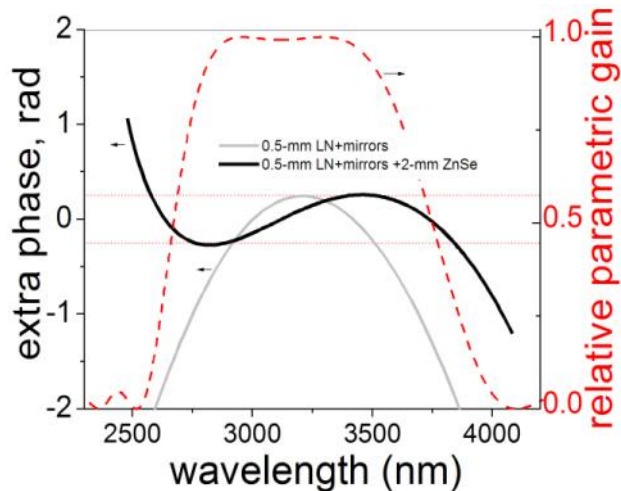


Fig. 4. Computed extra phase accumulated per cavity roundtrip due to the dispersion of 0.5-mm PPLN plus mirrors (gray curve) and (black curve) with ZnSe added for dispersion compensation. Horizontal dotted lines indicate calculated tolerance of the OPO for extra phase. Dashed line indicates parametric gain curve for the 0.5-mm PPLN.

The 2<sup>nd</sup> order interferometric autocorrelation of the OPO output was measured with a Michelson interferometer and an 'extended' InGaAs photodiode ( $\lambda < 2.2 \mu\text{m}$ ) serving as a 2-photon detector. The FWHM of the autocorrelation trace is 128 fs (Fig. 5) indicating a mid-IR pulse length of 91 fs (9 optical cycles) assuming a *sech*<sup>2</sup> pulse shape. In theory, the bandwidth of our generated frequency comb may support pulses as short as 3 cycles. Longer than expected pulse duration may be accounted for by spectral non-uniformity in the two-photon response of the detector as well as a substantial group dispersion introduced by a 1.5-mm-thick germanium substrate of our long pass filter (GVD of Ge is 1510 fs<sup>2</sup>/mm near 3  $\mu\text{m}$ ).

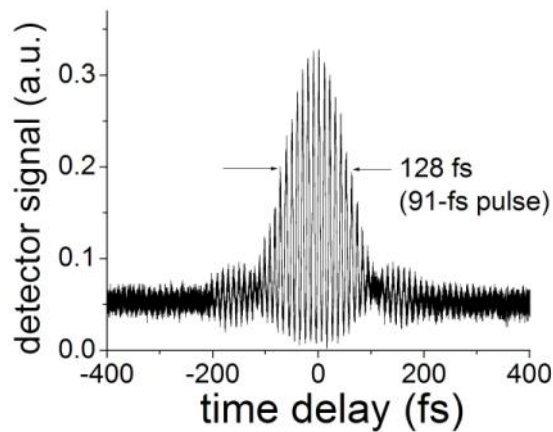


Fig. 5. Second-order autocorrelation trace measured via two-photon detection. The 128-fs FWHM of the trace suggests pulse length of 91 fs.

Our experimental results indicate that the output of our OPO is phase- and frequency-locked to the pump laser [20]. Stable interference fringes are observed when the outputs of two identical (but distinct) OPOs, pumped by the same fiber laser, are combined. The study of coherence properties of our OPO will be the subject of a separate paper. Briefly, there are two solutions [17] for the frequency comb 'teeth', given by  $\nu_n = f_{\text{CEO}}/2 + n f_{\text{rep}}$ , or  $\nu_n = f_{\text{CEO}}/2 + (n + 1/2) f_{\text{rep}}$  (here  $f_{\text{rep}}$  is the laser repetition frequency,  $f_{\text{CEO}}$  is the carrier-envelope offset

frequency of the pump laser, and  $n$  is the mode number). We were able to deterministically choose between these frequency states by manipulating the cavity length. Hence, our frequency comb mid-IR source is CEO-stabilized as long as the pump laser is CEO-stabilized.

#### **4. Conclusion**

In conclusion, we have shown that a broadband degenerate OPO is a simple, robust system with great promise for broadband wavelength conversion of near-IR frequency combs to the mid-IR. The broad spectral output we have achieved covers 2/3 octave from 2500 to 3800 nm – a range where OH, CH and NH chemical bonds show their strongest vibrational signatures. An octave-wide spectrum can be attained with more pump laser power, shorter PPLN crystals, and proper intracavity dispersion management using chirped mirrors. In addition, because the phase of our OPO is locked to that of the pump laser through the degenerate wavelength conversion process, this technique is especially suitable for extending coherent Fourier transform spectroscopy methods, including dual comb techniques, to the mid-infrared. Photon conversion efficiency of 40% can be further improved by purging the system and thus eliminating intracavity absorption by water vapor and CO<sub>2</sub>, and also by reduced mirror loss. Finally, our approach is very naturally extended to *cascaded* frequency comb generation, e.g. using an orientation-patterned GaAs in a second frequency-divide-by-two stage.

#### **Acknowledgments**

The authors thank Tim Brand for fabricating PPLN crystals designed for operation at Brewster angle. We gratefully acknowledge support from the US Office of Naval Research (ONR), NASA, Air Force Office of Scientific Research (AFOSR), Agilent Technologies and Stanford Medical School.